Dual Coupler Configuration at DSS 14 for the Voyager Era

T. Y. Otoshi, K. B. Wallace, and R. B. Lyon
Radio Frequency and Microwave Subsystems Section

This article describes the dual coupler configuration which was recently installed at DSS 14 for station delay calibrations during the Voyager era. The Z-correction values determined for this new and previous configurations are presented.

I. Introduction

During the antenna down time at DSS 14 (April-June 1977), a new S-band WR430 waveguide coupler was installed near the input to the S-Band Polarization Diversity (SPD) feed as shown in Fig. 1. This waveguide coupler, referred to as the "dual coupler," samples the uplink S-band signal and injects the translated downlink S-band signal on opposite walls of the WR430 waveguide coupler at basically the same point in the system. The dual coupler is used with the Block 4 translator for purposes of station delay calibrations. Each coupling arm of the dual coupler is a compact loop coupler assembly (actual length less than 5 cm) and has a coupling value of 54 dB and 25 dB minimum directivity. The dual coupler is water-cooled and able to pass 400 kW of CW power without arcing.[1]

There are several advantages to this new configuration. One main advantage is that the sampling-injection points are both close to the feed horn (see Fig. 1), so the same S-band Z-corrections (Ref. 1) apply whether you are using the SPD maser, Mod III maser, or the maser bypass mode. This reduces calibration measurements and bookkeeping problems by a factor of three. The second main advantage is that the diplexer and MTF filter delays no longer have to be precalibrated as was done in Ref. 2. Accuracy is improved because measurement errors of the diplexer and filter delays are eliminated. It is no longer necessary to assume that these component delays are frequency insensitive or stable with time, or that they are the same at all stations. The third advantage is that for this new dual coupler location near the feed horn, there are almost no WR430 waveguide delays that need to be calculated. This configuration currently appears to be the best compromise between having most of the desirable features of a dish-mounted zero delay device (ZDD) such as on 26-m antennas, and yet not having the undesirable features such as 64-m antenna multipath errors.

As discussed in Ref. 1, Z-corrections are necessary for correcting the measured ground station delays and referring them to the DSS reference location. This information is needed for determining the true range to the spacecraft. The new Z-corrections for this new configuration were determined from the same basic equation derived in Ref. 1 for the Block 4 Translator Method. This equation is:

$$Z = \tau_{\mathrm{XLTR}} - \sum_{i=3}^{6} \tau_i \qquad (1)$$

where τ_{XLTR} is the delay of the translator path between the uplink sampling point and the downlink injection point. The

[1]The dual coupler is discussed elsewhere in this volume by K. Wallace.

term τ_3 is the microwave delay from the uplink sampling point to the transmit horn phase center, and τ_4 is the microwave delay from the receive horn phase center to the downlink injection point. The terms τ_5 and τ_6 are, respectively, the uplink and downlink airpath delays from the horn phase centers to the DSS reference location via the convoluted Cassegrain antenna optics paths. These terms are defined more clearly and precisely in Ref. 1. The purpose of this article is to document the Z-correction determination method, the measured translator path delay values, and theoretical constants which will be useful for future reference and comparison purposes.

II. Translator Path Delay Measurement

As may be seen in Eq. (1), one of the terms needed to determine the Z-correction is the translator path delay τ_{XLTR}. This term includes the delays of the Level Set Attenuator Assembly, Block 4 Translator Assembly, Test Signal Control Assembly, and interconnecting cables. Because of the complexity of this path, this delay is measured rather than calculated. The translator path for the dual coupler configuration is basically the same as before (Ref. 3) except for the new locations of the sampling-injection points, which are now ports on the dual coupler near the feed horn (See Fig. 1). Due to new interconnecting cables that were installed for this new configuration, the translator path delay needed recalibration. The measurement procedure for its calibration is identical to that described previously (Ref. 3) with the exception that the sampling-injection points are different.

As described in Ref. 3, a portable zero delay device and its cables are substituted for the Block 4 translator path, and the range delay D_{ZDD} is measured. Then the ZDD cables are inserted in series with the Block 4 translator path, and the range delay is again measured and denoted as D'_{XLTR}. The measured translator delay is calculated from

$$(\tau_{XLTR})_m = D'_{XLTR} - D_{ZDD} + \tau_{ZDD} \qquad (2)$$

where τ_{ZDD} is the delay of the portable ZDD without its external cables. This value of τ_{ZDD} is known and had been precisely precalibrated in the laboratory. Equation (2) results in a measured value of the translator path between coaxial connection points to which the ZDD cables can be conveniently connected. However, the actual translator path must be defined internal to the waveguide system to points common to the "range on spacecraft path." Therefore small corrections need to be applied to measured values for the additional lengths of coax to waveguide paths involved. The true translator path delay is determined from the expression

$$\tau_{XLTR} = (\tau_{XLTR})_m + \tau_{WG,up} + \tau_{WG,down} \qquad (3)$$

The term $\tau_{WG,up}$ is a small correction term needed to go from the actual measurement uplink sampling point to the same point to where τ_3 is defined. The term $\tau_{WG,down}$ is a small correction term needed to go from the actual measurement downlink sampling point to the same point where τ_4 is defined.

Because the sampling-injection points are now located at the same plane for the dual coupler, the terms τ_3, τ_4, and τ_{XLTR} have a convenient common reference plane. This reference plane is the WR430 flange on the "dual coupler" assembly, which is connected to port K of the WR430 waveguide switch SW3 shown in Figs. 2 and 3. For the X-band downlink path, τ_4 and τ_{XLTR} are defined up to the midpoint of the X-band waveguide coupler installed directly in front of the X-band receive only (XRO) maser. For X-band the last coaxial connection point is the input to the XRO noise box, and the correction term $\tau_{WG,down}$ is the additional delay of the waveguide run through the XRO noise box assembly to the midpoint of the X-band waveguide coupler.

The translator delays measured at DSS 14 during July-August 1977 are shown in Table 1. There were more scatter and cyclic variations (±3 ns peak) in the measured translator path delays than were observed in the past. It is not clear whether this was due to a measurement problem (leakage in the ZDD cables or bad connectors) or due to an actual system leakage problem. Averaging the data at each channel over several test periods showed that the delay of the translator was essentially the same for Channels 9, 14, 18, and 22. Therefore an overall average was taken of the data to provide a best nominal value for the Voyager and Viking missions.

The corrected translator path delay values as well as values of $\tau_{WG,up}$ and $\tau_{WG,down}$ are tabulated in Table 2. For comparison purposes, the τ_{XLTR} values of the previous DSS 14 translator path delays are also shown.

III. Determinations of Theoretical Delays

As may be seen in Eq. (1), the Z-correction requires not only knowledge of τ_{XLTR} but also of τ_3, τ_4, τ_5, and τ_6. In contrast to determination of τ_{XLTR}, which is a measured value, the $\tau_3, \ldots, \tau_6$ are theoretical delays[2] calculated from physical dimensions and theoretical group velocities. These calculated delays are assumed to be constant with time and constant over the bandwidths of interest.

[2] In the previous configurations at DSS 14, some of the component delays of τ_3 and τ_4 had to be determined through measurements (Ref. 2).

The values of the individual component delays of τ_3 and τ_4 are shown tabulated in Figs. 2 and 3 for S-band. Some of these component delay values have been recalculated using computer programs and are slightly different from those reported previously in internal JPL reports. However, with the exception of the feed horn delays, the differences are small. The major changes in τ_3 and τ_4 for S-band are due to the new locations of the sampling-injection points.

The values of τ_5 and τ_6, which are theoretical airpath delays, did not change for the S-band uplink and downlink airpaths. For the X-band system, installation of new components in the XRO feed assembly has caused changes in the downlink values of τ_4 and τ_6 for X-band. These changes have been pointed out by Buchanan (Ref. 4), and individual component delays of τ_4 were recomputed and tabulated as shown in Table 3.

IV. Z-Corrections

The final Z-corrections for the new dual coupler configurations are computed and shown in Table 4. For comparison purposes, the old values are also shown. It can be seen that the major differences in the old and new Z-corrections are in the τ_3 and τ_4 values due to the new locations of the sampling-injection points. As shown in Table 4, the new Z-corrections for DSS 14 are currently

$$Z_s = [-38.83 \pm 0.99\,(1\sigma)] \text{ ns}$$

$$Z_x = [-48.67 \pm 0.94\,(1\sigma)] \text{ ns}$$

The 1σ errors shown for the Z-corrections are estimates based on translator delay measurement standard deviations, tolerances on the delay of the portable ZDD used as the calibration standard, and also tolerances on the theoretical $\tau_3, \ldots, \tau_6$ delay values. These individual error sources and estimated error contributions are shown in Table 5. The lists of error sources do not include waveform distortion. This is presently a source of error that has not been investigated by this author, and the effects on calibration accuracy are not presently known. The methods described by Komarek (Ref. 5), however, have been applied to correct and minimize possible waveform distortion errors.

Acknowledgements

M. Franco of Section 333 assisted with the experimental work. The implementation of the dual coupler configuration at DSS 14 was encouraged and supported by C. Stelzried and B. Seidel for the Voyager Project. H. Buchanan and D. Bathker provided most of the information needed to determine the theoretical delays through the feed assemblies.

References

1. Komarek, T., and Otoshi, T., "Terminology of Ranging Measurements and DSS Calibrations," in the *Deep Space Network Progress Report 42-36,* pp. 35-40, Jet Propulsion Laboratory, Pasadena, Ca., Dec. 15, 1976.

2. Lay, R., "Phase and Group Delay of S-Band Megawatt Cassegrain Diplexer and S-Band Megawatt Filter," in the *Deep Space Network Progress Report 42-37,* pp. 198-203, Feb. 15, 1977.

3. Otoshi, T. Y., Batelaan, P. D., Wallace, K. B., and Ibanez, F., "Calibration of Block 4 Translator Path Delays at DSS 14 and CTA 21," in the *Deep Space Network Progress Report 42-37,* pp. 188-197, Feb. 15, 1977.

4. Buchanan, H., private communication.

5. Komarek, T., private communication.

Table 1. Measured translator path delays via dual coupler configuration

Channel	Using new portable ZDD			Using crystal mixer ZDD	Average at each channel, ns
	Jul 17, 1977, ns	Aug 8, 1977, ns	Aug 9, 1977, ns	Aug 9, 1977, ns	
(S,S) translator path					
9	203.4	212.8	[210.1 203.6]	203.5	206.68 ± 1.99 (1σ)
14	208.2	209.0	208.2	205.0	207.60 ± 1.77 (1σ)
18	202.0	209.1	205.9	[211.7 210.7]	207.88 ± 1.77 (1σ)
22	207.6	206.4	202.3	211.3	206.90 ± 1.85 (1σ)
Avg.	205.3	209.3	206.0	208.4	
Overall average of $(\tau_{XLTR,S})_m$ = [207.3 ± 0.80 (1σ)] ns					
(S,X) translator path					
9	172.7	168.6	168.0		169.77 ± 1.47 (1σ)
14	169.6	168.4	172.2		170.07 ± 1.12 (1σ)
18	171.2	167.5	[169.0 167.0]		168.68 ± 1.89 (1σ)
22	162.2	167.9	164.5		164.87 ± 1.66 (1σ)
Avg.	168.9	168.1	168.1		
Overall average of $(\tau_{XLTR,X})_m$ = [168.4 ± 0.80 (1σ)] ns					

Table 2. Comparisons of old and new translator path delays at DSS 14

Config.[a]	$(\tau_{XLTR})_m$, ns	$\tau_{WG,up}$, ns	$\tau_{WG,down}$, ns	τ_{XLTR}, ns
(S,S) translator path				
Old config. Viking era Ch 17	187.78	0.0	2.46	190.24
New config. Voyager era Ch 9 → 22	207.3 (from Table 1)	0.42	0.41	208.13
(S,X) translator path				
Old config. Viking era Ch 17	177.04	0.0	6.01	183.05
New config. Voyager era Ch 9 → 22	168.4 (from Table 1)	0.42	6.01	174.83

[a]Old configuration data applicable from Dec. 17, 1975 to April 1977. New configuration data applicable from June 1977 to present.

Table 3. Group delay of XRO cone feed assembly with RCP/LCP select feature

Feed part	Length, cm (in.)	λ_{co}, cm (in.)	ns/cm (in.)	τ_g, ns[a]
Horn	*	*		2.07
#1 rotary joint	10.160 (4.000)	5.933 (2.336)	0.04169 (0.1059)	0.4236
#2 rotary joint	10.160 (4.000)	5.933 (2.336)	0.04169 (0.1059)	0.4236
Polarizer	10.452 (4.115)	5.761 (avg) (2.268)	0.04244 (0.1078)	0.4436
Cosine taper	12.700 (5.000)	6.142 (2.418)	0.04094 (0.1040)	0.5200
W.G. switch	8.484 (3.340)	6.350 (2.500)	0.04028 (0.1023)	0.3417
W.G. elbow	13.970 (5.500)	6.350 (2.500)	0.04028 (0.1023)	0.5627
Adaptor	1.097 (0.432)	6.015 (2.368)	0.04138 (0.1051)	0.0454
New W.G. spacer	6.020 (2.370)	5.933 (2.336)	0.04169 (0.1059)	0.2510
WR112 to mid-point of coupler	6.033 (2.375)	5.700 (2.244)	0.04272 (0.1085)	0.2577
			Total delay =	5.3393

[a]Calculated at 8420 MHz. Data obtained from internal JPL report by H. Buchanan.

Table 4. Comparisons of old and new theoretical constants and Z-corrections for DSS 14

(S,S) translations

Configuration	$\tau_{XLTR,S}$, ns	Waveguide[a]		Airpath		$\sum_{3}^{6} \tau_i$, ns	Z_S, ns
		τ_3, ns	$\tau_{4,S}$, ns	τ_5, ns	$\tau_{6,S}$, ns		
Old config. Viking era Ch 17	190.24 (from Table 2)	62.32	45.88	102.56	102.56	313.32	-123.08
New config. Voyager era Ch 9 → 22	208.13 (from Table 2)	22.18	19.66	102.56	102.56	246.96	-38.83
Difference	-17.89	40.14	26.22	0.00	0.00	66.36	-84.25

(S,X) translations

Configuration	$\tau_{XLTR,X}$, ns	Waveguide[b]		Airpath		$\sum_{3}^{6} \tau_i$, ns	Z_X, ns
		τ_3, ns	$\tau_{4,X}$, ns	τ_5, ns	$\tau_{6,X}$, ns		
Old config. Viking era Ch 17	183.05 (from Table 2)	62.32	6.08	102.56	93.62	264.58	-81.53
New config. Voyager era Ch 9 → 22	174.83 (from Table 2)	22.18	5.34	102.56	93.42[c]	223.50	-48.67
Difference	8.22	40.14	0.74	0.00	0.20	41.08	-32.86

[a]New values of τ_3 and $\tau_{4,S}$ calculated in Figs. 2 and 3.

[b]New value of $\tau_{4,X}$ given in Table 3.

[c]New value of $\tau_{6,X}$ shortened by 0.2 ns per H. Buchanan (Ref. 4).

Table 5. Estimated error contributions for *Z*-corrections for dual coupler configuration

Parameter	S-band (1σ) tolerances, ns	X-band (1σ) tolerances, ns
$\tau_3 + \tau_4$ values	±0.5	±0.4
τ_{ZDD}	±0.2	±0.2
$\tau_5 + \tau_6$	±0.2	±0.2
$\tau_{WG,up} + \tau_{WG,down}$	±0.1	±0.1
Measurement scatter on τ_{XLTR}	±0.80 (see Table 1)	±0.80 (see Table 1)

Total error = $\sqrt{[\Sigma\sigma^2]}$

= 0.99 ns for S-band *Z*-correction

= 0.94 ns for X-band *Z*-correction

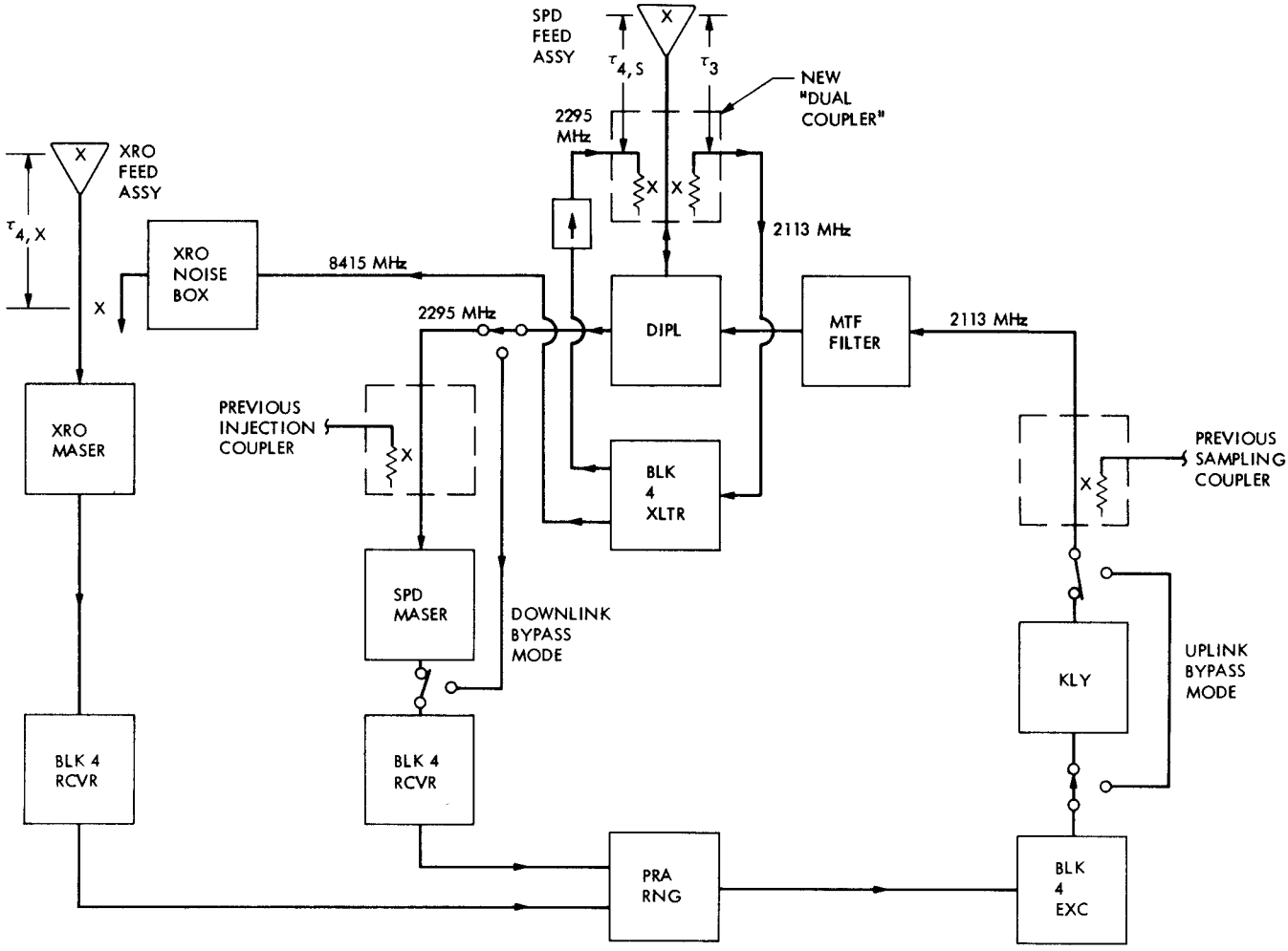

Fig. 1. Simplified block diagram of new dual coupler DSS 14 range calibration configuration

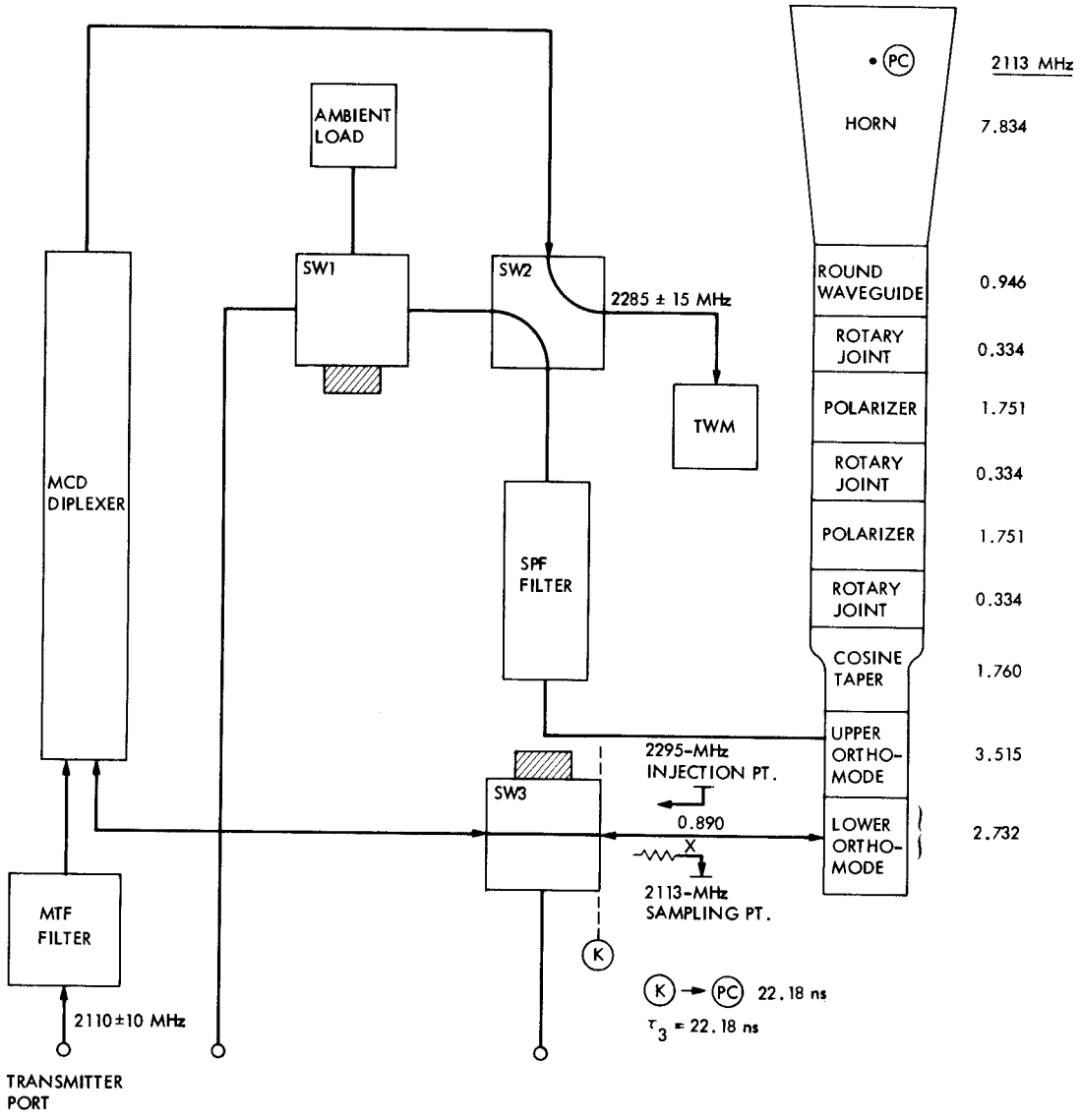

Fig. 2. Block diagram of SPD feed horn assembly and values of component delays for τ_3 at S-band

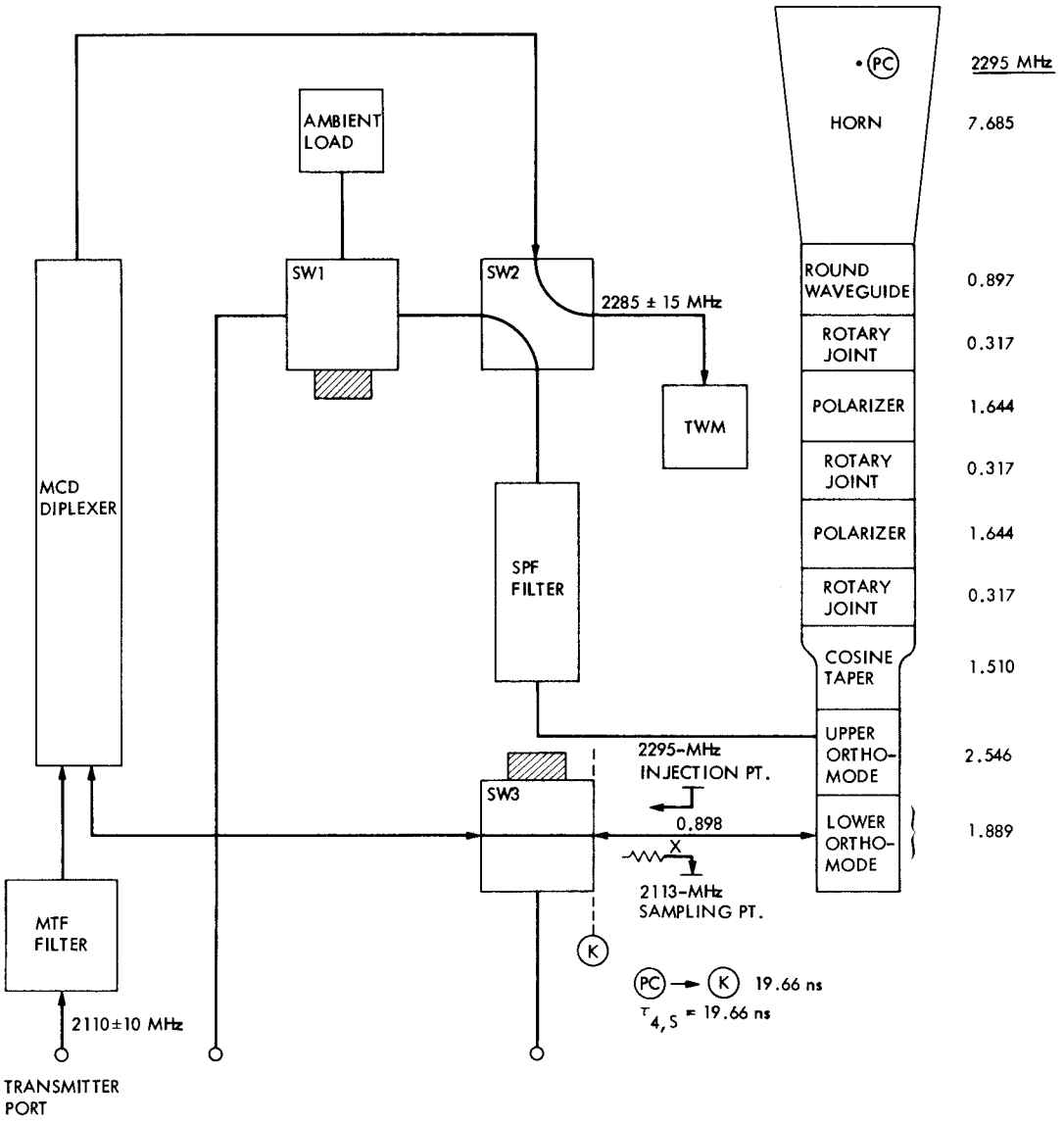

Fig. 3. Block diagram of SPD feed horn assembly and values of component delays for τ_4 at S-band